Ab initio calculations on aluminosilicate Q^3 species: Implications for atomic structures of mineral surfaces and dissolution mechanisms of feldspars

J.D. KUBICKI,[1] G.A. BLAKE,[2] AND S.E. APITZ[1]

[1]Remediation Research Laboratory, Chemistry and Biochemistry Branch, NCCOSC RDT&E Div 361,
53475 Strothe Road, Room 258, San Diego, California 92152–6325, U.S.A.
[2]Division of Geological and Planetary Sciences, California Institute of Technology, 170–25, Pasadena, California 91125, U.S.A.

ABSTRACT

Molecular orbital calculations on various aluminosilicate Q^3 T-OH and bridging O species were performed to model atomic structural changes on mineral surfaces that occur as a function of pH. Calculated vibrational frequencies are reported for the terminal T-O, T-OH, and O-H bonds of the central T cation as a test of our models, and the predicted frequencies compare well with experimental vibrational spectra of aluminosilicates. Optimized bond lengths and T-O-T angles to the central Q^3 Si^{4+} and Al^{3+} cations in these molecules change significantly as the T-OH bond is protonated and deprotonated. Protonation of terminal bonds tends to shorten and strengthen the remaining three $T-O_{br}$ bonds that would attach the central cation to the bulk mineral. This result is in contrast to the $T-O_{br}$ weakening that has been suggested previously as a mechanism for proton-assisted dissolution (e.g., Furrer and Stumm 1986; Wieland et al. 1988). Proton affinities (PA) of the Q^3 T-OH, $T-OH_2$, and T-OH-T species are predicted to help delineate the process of proton-assisted dissolution in quartz and feldspars. Theoretical results predict that the PAs of $Al-OH_2$ and Al-OH-Si species are comparable; thus, as $Al-OH_2$ surface species become stable, protons are also energetically favored to attach to bridging O atoms. In addition, we found that substitution of Al^{3+} for Si^{4+} in the second-nearest-neighbor site of a Q^3 Si-OH can increase the calculated PA, although the effect is diminished by the presence of a charge-balancing Na^+ cation. This result has implications for models that attempt to describe the behavior of aluminosilicate surfaces in terms of the component oxides. Addition of Na^+ to charge balance molecules strongly affects calculated structures, proton affinities, and vibrational spectra. The role of charge-balancing cations was often omitted in previous theoretical studies of aluminosilicates, but the magnitude of the charge-balancing effect could alter the results and conclusions of earlier calculations in this area.

INTRODUCTION

Terminal cation-O bonds (X-O) on the surfaces of aluminosilicate and oxide minerals are believed to undergo hydrolysis reactions, such as

$$XO^- + H^+ \rightleftharpoons XOH \qquad (1)$$

$$XOH + H^+ \rightleftharpoons XOH_2^+ \qquad (2)$$

as a function of the ambient solution pH [Westall (1987) and references therein]. Surface-speciation changes may affect the terminal X-O bond strengths and the bond strengths of the surface cation to the bulk mineral (e.g., Furrer and Stumm 1986; Wieland et al. 1988; Brady and Walther 1989; Lasaga 1992). In addition, reactions at bridging O sites may also occur, resulting in the formation of T-OH-T sites or hydrolysis of T-O-T linkages (Xiao and Lasaga 1995). These changes are important because the atomic surface structure of a mineral often controls the kinetics of water-rock reactions [see Hochella

and White (1990) for a recent review]. However, because these changes occur on the surface of the mineral grain, direct experimental determination of their atomic structures is difficult.

This theoretical investigation of some possible mineral-surface atomic structures employed calculations on Q^3 species (where Q^n indicates the number of bridging O atoms per tetrahedral cation; see Kirkpatrick 1988) as models for the local atomic structure of tetrahedral cations on mineral surfaces. Absolute values of structural parameters and reaction energetics may be somewhat different in model molecules and mineral surfaces because of the neglect of crystal-structure constraints and solvation effects; hence, we focused on relative changes in structure and energy associated with protonation and deprotonation of the molecules, which should be similar on mineral surfaces. Theoretical structure and PA changes were then used to rationalize observed dissolution rates of minerals as a function of pH.

Although octahedral cations play a significant role in sorption and dissolution phenomena in many minerals such as clays and aluminum hydroxides (Schulthess and Huang 1991), in minerals such as quartz and feldspars various species of tetrahedral Si^{4+} and Al^{3+} are thought to dominate surface reactions (Blum and Lasaga 1988; Hellmann et al. 1990). Furthermore, end-member minerals (e.g., SiO_2 and γ-Al_2O_3) are often used as analogs for the Si^{4+} and Al^{3+} components in aluminosilicate mineral-surface reactions (Parks 1967), but it has not been shown that Si^{4+} and Al^{3+} behave identically in the end-member and aluminosilicate minerals with respect to surface chemistry. Recent infrared spectra (Koretsky et al., in preparation) suggest that this assumption may be invalid. Hence, we tested the oxide component model by comparing theoretical predictions on the structures and vibrational spectra of Q^3 Si with three second-nearest-neighbor Si^{4+} ions (i.e., a silica model) vs. Q^3 Si with two second-nearest-neighbor Si^{4+} ions and one Al^{3+} ion (i.e., an albite model).

Different types of surface OH groups (or the absence thereof) have varying effects on the reactivity of mineral surfaces (Schindler and Stumm 1987). For example, adsorption equilibria of metals (e.g., Balistrieri and Murray 1984) and organic molecules (e.g., Zachara et al. 1994) onto mineral surfaces vary as a function of pH. Infrared spectroscopy has been used to identify surface OH groups experimentally for many years (for reviews see Boehm 1966; Fripiat 1982). Hence, correct assignments of the OH vibrational bands in aluminosilicate minerals are important for understanding mineral-surface chemistry. We report theoretical vibrational frequencies, infrared activities, and Raman intensities of the T-O and O-H stretching modes in our model Q^3 Si and Al molecules as tests of previous assignments and predictions.
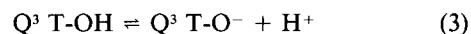
CALCULATION DETAILS

The program Gaussian 92 with a standard 3-21G** basis set (Frisch et al. 1992) was used to calculate the structures, potential energies, and vibrational frequencies of model terminal O sites: $\{[(OH)_3SiO]_3SiO\}^{1-}$, $[(OH)_3$-$SiO]_3Si(OH)$, $\{[(OH)_3SiO]_2(OH)_3AlOSiO\}^{2-}$, $\{[(OH)_3$-$SiO]_2(OH)_3AlOSi(OH)\}^{1-}$, $Na^+[(H_3SiO)_2H_3AlOSiO]^{2-}$, $Na^+[(H_3SiO)_2H_3Al$-O-$SiOH]^{1-}$, $\{[(OH)_3SiO]_3AlO\}^{2-}$, $\{[(OH)_3SiO]_3Al(OH)\}^{1-}$, $[(OH)_3SiO]_3Al(OH_2)$, $[(H_3SiO)_3$-$AlO]^{2-}$, $[(H_3SiO)_3AlOH]^{1-}$, $Na^+[(H_3SiO)_3AlO]^{2-}$, $Na^+[(H_3SiO)_3Al(OH)]^{1-}$, $Na^+[(H_3SiO)_3Al(OH_2)]$. In addition, bridging O sites were also modeled: $H_6Si_2O_7$, $(H_7Si_2O_7)^+$, $(H_6SiAlO_7)^{1-}$, H_7SiAlO_7, $Na^+(H_6SiAlO_7)^{1-}$, and $Na^+(H_7SiAlO_7)$. {The above molecules are hereafter designated $(Si_3)Si$-O, $(Si_3)Si$-OH, $(Si_2Al)Si$-O, $(Si_2Al)Si$-OH, $Na^+[(HSi_2Al)Si$-$O]$, $Na^+[(HSi_2Al)Si$-$OH]$, $(Si_3)Al$-O, $(Si_3)Al$-OH, $(Si_3)Al$-OH_2, $(HSi)_3Al$-O, $(HSi)_3Al$-OH, $Na^+(HSi)_3Al$-O, $Na^+(HSi)_3Al$-OH, $Na^+(HSi)_3Al$-OH_2, Si-O-Si, Si-OH-Si, Al-O-Si, Al-OH-Si, Na^+Al-O-Si, and Na^+Al-OH-Si, respectively.}

Q^3 species should be reasonable models for aluminosilicate surface groups because they include bonding similar to minerals out to third-nearest neighbors. Other models, such as the double four-membered ring cluster used in Sauer and Hill (1994), may unnecessarily restrict relaxation owing to symmetry constraints. In addition, optimized structures (e.g., T-O_{br} bond lengths and T-O-T angles) of four-membered aluminosilicate rings are significantly different from molecules with other ring structures or those not in rings (Kubicki and Sykes 1993; Sykes and Kubicki 1996); hence, results based on the double four-membered ring model may not be as relevant to mineral surfaces where other intermediate range structures are present.

The 6-311+G** basis set, which employs a large triple-split valence with diffuse functions (+) and higher angular-momentum quantum-number orbitals on all atoms (** = 3d for O, Al, and Si, and 2p for H) to account for polarization (Hehre et al. 1986; Frisch et al. 1992), was used to calculate potential energies at the optimized 3-21G** geometries (i.e., 6-311+G**//3-21G**). Molecular potential energies plus the 3-21G** zero-point vibrational energies (ZPEs) were used to estimate PAs (Brand et al. 1993) from reactions of the type

$$Q^3 \text{ T-OH} \rightleftharpoons Q^3 \text{ T-O}^- + H^+ \qquad (3)$$

and

$$Q^3 \text{ T-OH}_2^+ \rightleftharpoons Q^3 \text{ T-OH} + H^+. \qquad (4)$$

Vibrational frequencies reported in this paper are scaled by 0.89 to account for anharmonic effects, the neglect of electron correlation, and limitations of the basis set (Pople et al. 1981). Although the 3-21G** basis does not produce accurate absolute frequencies, frequency shifts with structure can be reliably compared to experimental values (Kubicki et al. 1993a; Kubicki and Sykes 1993; Sykes and Kubicki 1996). Thus, these predicted frequencies can be used to help interpret changes in vibrational spectra as a function of pH.

$(Si_3)Al$-O was optimized with constrained O-H bond lengths and H-O-Si-O_{br} dihedral angles on the external tetrahedra because this molecule is energetically unstable in our calculations relative to a configuration with one H^+ from an Si-OH linkage hopping to the Al-O group, thereby forming an Al-OH and an Si-O bond. (This transfer occurred during the full optimization of the molecule and led to a decrease in the potential energy of $\approx$ -250 kJ/mol.) Consequently, vibrational frequencies were not calculated for $(Si_3)Al$-O. The ZPE for this species was estimated by subtracting the difference between the Q^3 Al-OH and Q^n Al-OH_2 ZPEs (approximately 30 kJ/mol) from the Q^3 Al-OH ZPE. When we used this approximation with the molecules $(H_3SiO_4)^-$, H_4SiO_4, and $(H_5SiO_4)^+$, the estimated ZPE for $(H_3SiO_4)^-$ is within 1 kJ/mol of the calculated value. The difference between the calculated ZPEs for $(H_3SiO_4)^-$ and H_4SiO_4 = 32 kJ/mol, for H_4SiO_4 and $(H_5SiO_4)^+$ = 33 kJ/mol, and for Q^3 Al-OH and Q^3 Al-OH_2 = 35 kJ/mol. These values are all similar to the ZPE correction of 29–32 kJ/mol for an O-H bond as calculated by Fleischer et al. (1993).
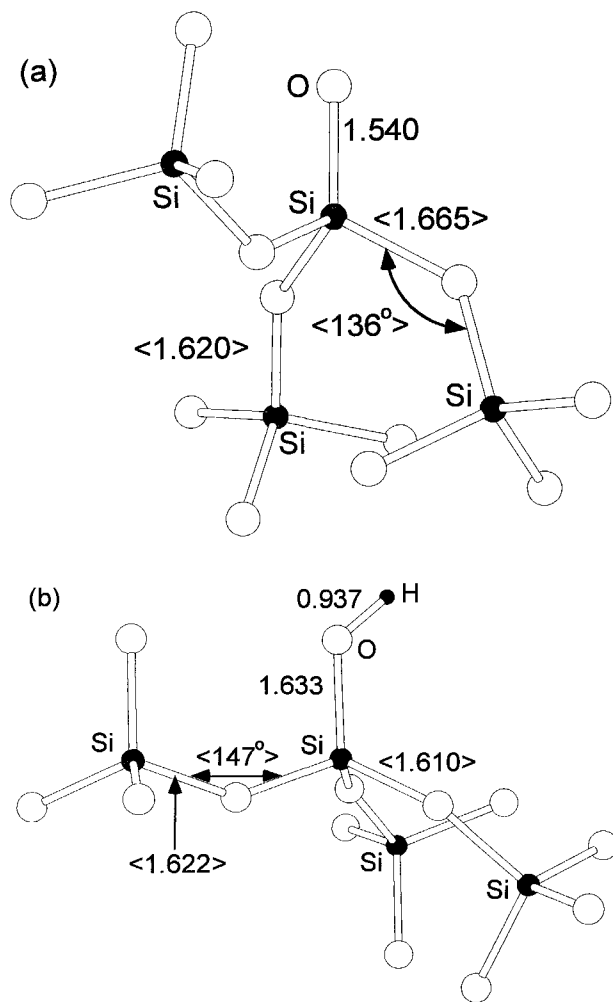
FIGURE 1. Predicted structures of (a) $(Si_3)Si$-O and (b) $(Si_3)Si$-OH minimum potential energy configurations with the 3-21G** basis set. Atoms are coded according to H = black, O = white, Si = dark gray. Bond lengths are in angstroms and angles in degrees. H atoms on external tetrahedra are not included for clarity in the figure but were included in the calculations. The angle brackets indicate an average bond length or angle of a particular type. Structural parameters can be cross-referenced in Table 1. Molecules drawn with the program Atoms (Dowty 1993).

TABLE 1. Calculated structural parameters of the molecules

Molecule	T-O (Å)	T-OH (Å)	T-O$_{br1}$ (Å)	T-O$_{br2}$ (Å)	O-H (Å)	T-O-T (°)
$(Si_3)Si$-O	1.540		1.665	1.620		136
$(Si_3)Si$-OH		1.633	1.610	1.622	0.937	147
$(Si_3)Si$-OH*		1.540	1.665	1.620	0.937	136
$(Si_2Al)Si$-O	1.539		1.695**	1.617**		130**
			1.642†	1.766†		125†
$(Si_2Al)Si$-OH		1.635	1.628**	1.625**	0.937	145**
			1.589†	1.745†		140†
Na⁺[(HSi₂Al)Si-O]	1.526		1.718**	1.632**		127**
			1.610†	1.753†		169†
Na⁺[(HSi₂Al)Si-OH]		1.621	1.637**	1.642**	0.936	158**
			1.588†	1.799†		164†
$(Si_3)Al$-O	1.676		1.784	1.559		123
$(Si_3)Al$-OH		1.779	1.740	1.607	0.939	134
$(Si_3)Al$-OH₂		1.873	1.714	1.594	0.966	143
(HSi)₃Al-O	1.637		1.821	1.579		137
(HSi)₃Al-OH		1.733	1.743	1.587	0.937	172
Na⁺[(HSi)₃Al-O]	1.616		1.838	1.607		134
Na⁺[(HSi)₃Al-OH]		1.680	1.763	1.623	0.930	147
Na⁺[(HSi)₃Al-OH₂]		1.892	1.715	1.651	0.946	152

Note: T-O$_{br1}$ = distance from central T cation to bridging O atom; T-O$_{br2}$ = distance from external T cations to bridging O atoms.
* Constrained structure.
** Si⁴⁺ second-nearest neighbors.
† Al³⁺ second-nearest neighbors.

RESULTS

Structural changes with protonation

Calculated structures of $(Si_3)Si$-O and $(Si_3)Si$-OH are pictured in Figure 1, and selected structural parameters are listed in Table 1. The main result is that the terminal Si-O bond length increases by 6% from 1.540 to 1.633 Å as a proton is added to form Si-OH. This increase may be lessened if a hydrating H_2O molecule were included in the optimization because the Si-O bond in $(H_3SiO_4)^-$ increases from 1.537 to 1.551 Å (1%) with the addition of H_2O to form the dimer $(H_3SiO_4-H_2O)^-$ (Kubicki et al.

1993b). In addition, the Si-OH bond in H_4SiO_4 decreases from 1.629 to 1.615 Å (1%) in $H_4SiO_4-H_2O$ (optimized HF 6-31G* structure). Thus, for hydrated Si-O vs. Si-OH the bond-length difference may be closer to 1.615–1.551 = 0.064 or 4%. The calculations presented here more closely represent dehydrated surfaces after reaction with aqueous solutions.

Si-O$_{br}$ (O$_{br}$ = bridging O atom) bond lengths from the central Q^3 cation are also affected by protonation (Table 1 and Fig. 1b). The average Si-O$_{br}$ decreases by 3% because of the lengthening of the terminal Si-O bond. Thus, if the Si-O$_{br}$ bonds represent the linkages of a surface Si^{4+} to the bulk mineral, protonation of the Si-O surface group strengthens the attachment to the mineral. An increase of 11° in the average Si-O-Si angle also occurs in the protonated species in comparison with the deprotonated species. These calculated results probably overestimate the actual structural changes that occur on mineral surfaces because the molecular structures are allowed to relax fully. Full relaxation may not occur in minerals owing to restrictions of the surrounding structure (Brand et al. 1993). On the other hand, minerals undergoing dissolution may form an amorphous surface layer (Schulthess and Huang 1991) where structural relaxation readily occurs, so our models are better representations of a surface undergoing dissolution than they are representations of a pristine mineral surface.

Table 1 also contains structural parameters relevant to albite surface reactions from the molecules $(Si_2Al)Si$-O and $(Si_2Al)Si$-OH. Although the substitution of an Al^{3+} for an Si^{4+} in a second-nearest-neighbor site increases the net negative charge on the molecules in comparison with $(Si_3)Si$-O and $(Si_3)Si$-OH, only minor effects on the order

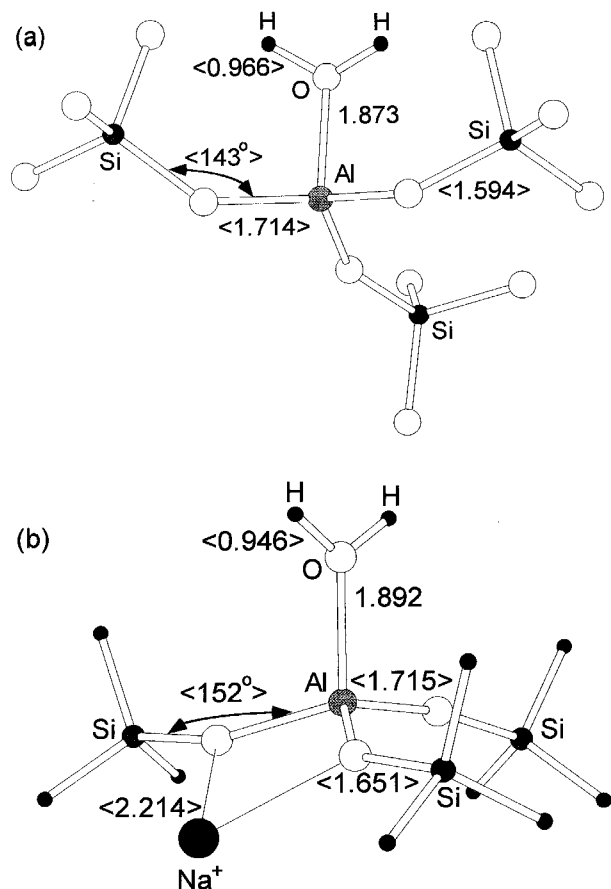FIGURE 2. Energy-minimized structure of (a) $(Si)_3Al-OH_2$ and (b) $Na^+[(HSi)_3Al-OH_2]$ with the 3–21G** basis set. In a and b, the bridging O atoms are fairly coplanar with the Al^{3+} atom in comparison with a regular tetrahedral configuration, which may allow direct attack by H_2O to form pentacoordinated Al^{3+}. Same legend as Figure 1, with Al in light gray and Na^+ in black. Bond lengths in angstroms and angles in degrees. H atoms on external tetrahedra in a were not included for clarity in the figure but were included in the calculations. Molecules drawn with the program Atoms (Dowty 1993).

of 0.1% are reflected in the terminal Q^3 Si-O, Si-OH, and O-H bonds; whereas, Si-O_{br} bond lengths change by 2% or more (Table 1). Hence, the excess negative charge on the molecule affects the Si-O_{br} bonds more strongly than the terminal Si-O and Si-OH bonds. Lengthening the Si-O_{br} bonds makes the T-O-T linkage more susceptible to hydrolysis and lowers the energy barrier to proton-assisted dissolution. Extrapolating these results to mineral surfaces suggests that Si^{4+} with at least one Al^{3+} second-nearest-neighbor site in feldspar minerals should more readily dissolve than Si^{4+} in quartz.

Examination of calculated results for Q^3 Al^{3+} species, listed in Table 1, reveals that surface protonation reactions can increase the terminal Q^3 Al-O bond length by 6% from $(Si_3)Al-O$ to $(Si_3)Al-OH$ and by 5% from $(Si_3)Al-OH$ to $(Si_3)Al-OH_2$ (Fig. 2). {The species $(Si_3)Al-(OH_3)^+$

is not likely to be stable because $[(OH)_3Al(OH_3)]^+$ optimizes to $Al(OH)_3 + H_3O^+$ during energy minimization.} Al-O_{br} bonds decrease by an average of 4%, and the Al-O-Si angles increase 16% from 123 to 143° between $(Si_3)Al-O$ and $(Si_3)Al-OH_2$. Both of these changes, shortening of the Al-O_{br} bonds and increasing of Al-O-Si angles, should tend to decrease the reactivity of the bridging O atoms connecting the Al^{3+} cation to the bulk mineral (Gibbs et al. 1981). Once again, these molecular clusters may overestimate the structural effects of protonation that actually occur on a mineral surface, but changes in the molecules and mineral surfaces should be qualitatively similar.

Cluster size and charge-balancing cation effects on molecular structure

Two model-dependent factors that may influence the accuracy of the above calculations when used as analogs of mineral surfaces are the size of the molecular cluster employed and the effect of Na^+ cations. Inclusion of Na^+ in the optimizations of $(Si_2Al)Si-O$, $(Si_2Al)Si-OH$, $(Si_3)Al-O$, $(Si_3)Al-OH$, and $(Si_3)Al-OH_2$ molecules would require an impractical increase in the amount of computational time necessary to determine a stationary point (i.e., an equilibrium structure or potential energy minimum). For this reason, we estimated the possible magnitudes of system-size and charge-balancing effects by optimizing Q^3 molecules with H^- anions substituted for $(OH)^-$ groups on the external (i.e., Q^1) tetrahedra both with and without Na^+ present.

To test the system-size effect, comparison of the $(HSi)_3Al-OH$ and $(Si_3)Al-OH$ molecules in Table 1 reveals that the most significant change is in the T-O-T angle. The OH-terminated molecule is predicted to have minimum-energy T-O-T angles much closer to those observed in minerals (Geisinger et al. 1985; Sharma et al. 1988). Another significant change is a 2.5% decrease in the Al-OH bond length associated with the central T cation. Because the OH-terminated molecule differs from the mineral-surface structure in the fourth-nearest-neighbor sites (i.e., substitution of a T cation for the H atom in each OH group), the system-size effect on the terminal T-O, T-OH, and T-OH_2 bonds in the OH-terminated molecules should be <2.5% compared with mineral-surface structures.

The second model-dependent effect on molecular structure, that of charge-balancing Na^+ cations, can be estimated by comparison of the $(HSi)_3Al-OH$ and $Na^+[(HSi)_3Al-OH]$ molecules. Again, the largest change noted is in the T-O-T angle as it decreases from 172 to 147° with addition of Na^+ (Table 1). The charge-balanced molecule gives the more accurate value for Si-O-Al angles in comparison with aluminosilicate minerals (Geisinger et al. 1985; Sharma et al. 1988) as the Na^+ interacts with all three bridging O atoms in the $Na^+[(HSi)_3Al-OH]$ molecule. (Note that in Fig. 2b the Na^+ interacts with only two bridging O atoms since the Na-O interaction is weakened by the change from negative to neutral charge ac-

companying protonation.) Bond lengths in the molecule all change with Na^+ addition as well. The largest shift is a 3% decrease in the Al-OH bond length associated with the central T cation (Table 1). These bond-length changes are probably caused by the large decrease in the calculated T-O-T angle because $T-O_{br}$ bond lengths are inversely correlated with T-O-T angles (Gibbs et al. 1981). Because the OH-terminated molecules already have smaller, more accurate T-O-T angles that are similar to those of $Na^+[(HSi)_3Al-OH]$, we consider the 3% difference in T-OH bond length between $(HSi)_3Al-OH$ and $Na^+[(HSi)_3Al-OH]$ to be a maximum for the possible effect of adding Na^+ to the OH-terminated molecules in Table 1.

Proton affinities of surface O sites in model quartz clusters

Table 2 lists the calculated energies and PAs for molecules examined in this study. If the inherent energetics of extracting protons from O sites in our model molecules can be related to protonation equilibria in minerals, then the sequence of elementary steps in the complex dissolution process should follow the order of decreasing PA (i.e., the sites with the highest PA protonate first as pH decreases). The PA of the $(Si_3)Si-OH$ group calculated from Equation 3 is 1429 kJ/mol. This PA is similar to the PA values of 1511 and 1474 kJ/mol for H_4SiO_4 with $6-311+G^{**}//3-21G^{**}$ and G2 theory calculations, respectively (Kubicki et al. 1995b, 1996). Other calculated values for the gas-phase PA of orthosilicic acid are 1565 kJ/mol with an HF 6-31G* basis set (O'Keeffe et al. 1985) and 1480 kJ/mol from density functional theory (Stave and Nicholas 1993). The cluster-size effect between H_4SiO_4 and $(Si_3)Si-OH$ is approximately 80 kJ/mol, when $6-311 +G^{**}//3-21G^{**}$ calculations on the two molecules are compared. Inclusion of MP2 electron correlation (Møller and Plesset 1934) has a comparable effect on calculated PAs. The difference between calculated PAs of H_4SiO_4 with HF 6-31G* and MP2 6-31G* basis sets is 35 kJ/mol (Kubicki et al. 1995a). Thus, cluster-size and basis-set effects do not play a dominant role in the calculated PA, but both may affect calculated energy changes by a few percent.

Fleischer et al. (1993) determined that basis-set limitations and neglect of electron correlation produces a systematic error of -33 ± 22 kJ/mol in PAs of OH groups. Adding this correction to our theoretical PA results in a PA of 1396 kJ/mol for a surface Si-OH. This calculated Q^3 Si-OH PA is in the experimental range of 1390 ± 25 kJ/mol for surface silanol groups (Paukshtis and Yurchenko 1983). Furthermore, the $(Si_3)Si-OH$ PA is equal to that calculated by Sauer and Hill (1994) for double four-membered ring clusters; hence, molecular structure beyond second-nearest neighbors does not have a significant effect on calculated PAs.

Some authors have treated surface speciation at mineral-water interfaces as an analog of aqueous-phase reactions for the same types of coordination polyhedra (e.g.,

TABLE 2. Calculated energies and proton affinities of various O sites on aluminosilicate surfaces

Molecule	Energy (Hartrees)	Proton affinity (kJ/mol)
Q^3 species		
$(Si_3)Si-O$	−2135.28671	
$(Si_3)Si-OH$	−2135.83117	1429(1390)[a]
$(Si_3)Si-OH^*$	−2135.78501	1308
$(Si_2Al)Si-O$	−2088.22438	
$(Si_2Al)Si-OH$	−2088.91269	1807
$Na^+[(HSi_2Al)Si-O]$	−1575.68174	
$Na^+[(HSi_2Al)Si-OH]$	−1576.24079	1468
$(Si_3)Al-O$	−2088.14364	
$(Si_3)Al-OH$	−2088.90675	2004
$(Si_3)Al-OH_2$	−2089.40836	1317
$(HSi)_3Al-O$	−1413.65358	
$(HSi)_3Al-OH$	−1414.42583	2028
$Na^+[(HSi)_3Al-O]$	−1575.65013	
$Na^+[(HSi)_3Al-OH]$	−1576.27376	1637
$Na^+[(HSi)_3Al-OH_2]$	−1576.64064	963
Other species		
H_4SiO_4	−590.97176	1511
$[(OH)_3Si(OH_2)]^+$	−591.26746	776
$Si(OH)Si$	−1106.21667	777
$Al(OH)Si$	−1059.47059	1301(1188–1330)[b]
$Na^+Al(OH)Si$	−1221.21220	954
H_2O	−76.03045	1665(1635)[c]
H_3O^+	−76.29483	694(697)[c]

Note: Energies calculated using $6-311+G^{**}//3-21G^{**}$ with $3-21G^{**}$ ZPE correction. Experimental values in parentheses.
* Constrained structure.
[a] Paukshtis and Yurchenko (1983).
[b] Datka et al. (1988).
[c] Lias et al. (1988).

$^{[6]}Al^{3+}_{surf} \approx {}^{[6]}Al^{3+}_{aq}$). For example, Schindler and Stumm (1987) noted that the log K_a values of many cations in the aqueous phase and at surface sites are correlated within one log unit. An important exception to this correlation is that log $K_a(H_4SiO_4)_{aq} = -10.07$ and log $K_a(SiO_2)_{surf} = -6.71$. Hence, a discrepancy exists in a proposed trend for one of the most important and common components in soils and sediments.

We hypothesized that the difference between H_4SiO_4 and surface Si-OH deprotonation may be caused by lattice restrictions on the relaxation of local structure surrounding terminal Si-OH bonds. Si^{4+} is different from most other elements used in the above correlation (Schindler and Stumm 1987) because it occurs nearly exclusively in tetrahedral coordination under low-pressure conditions. Furthermore, SiO_4 tetrahedra are an integral part of the framework structure in many silicates; hence, SiO_4 tetrahedral relaxation may be more restricted than relaxation in octahedral species owing to this polymerization.

To test this hypothesis, calculations were performed on the $(Si_3)Si-OH$ molecule in the $(Si_3)Si-O$ molecular structure with only the O-H bond length, Si-O-H angle, and O-Si-OH dihedral angle allowed to relax upon protonation [designated $(Si_3)Si-OH^*$ in Tables 1 and 2]. The calculated PA of the $(Si_3)Si-OH^*$ group is 121 kJ/mol less than when full structural relaxation was allowed (i.e., 1308

vs. 1429 kJ/mol; Table 2). Hence, the constrained $(Si_3)Si-OH^*$ group is more acidic than the fully relaxed $(Si_3)Si-OH$. Combined with the result that $6-311+G^{**}//3-21G^{**}$ calculations predict a PA for H_4SiO_4 that is 82 kJ/mol higher than that for $(Si_3)Si-OH$ (i.e., 1511 vs. 1429 kJ/mol; Table 2), the total ΔPA between the aqueous and surface species may be as high as 200 kJ/mol. This energy difference helps to explain the observed discrepancy between the $\log K_a(H_4SiO_4)_{aq}$ and the $\log K_a(SiO_2)_{surf}$.

If the change in ΔG between the aqueous and surface deprotonation reactions is ascribed solely to the difference in PAs of surface Si-OH vs. H_4SiO_4, then the ratio of PAs would be equal to $PA_{aq}/PA_{surf} = \Delta G_{aq}/\Delta G_{surf} = \log K_a(H_4SiO_4)_{aq}/\log K_a(SiO_2)_{surf} = -10.07/6.71 = 1.50$. If agreement to within only one $\log K_a$ unit is required, as found in Schindler and Stumm (1987), then PA_{aq}/PA_{surf} should be equal to approximately 1.31, but the calculated ratio of $PA_{aq}/PA_{surf} = 1511/1308 = 1.16$. A larger ΔS term for the release of a proton from a surface into aqueous solution in comparison with that for deprotonation of $(H_4SiO_4)_{aq}$ could lower $\Delta G_{aq}/\Delta G_{surf}$ further and bring the $\Delta G_{aq}/\Delta G_{surf}$ ratio into closer agreement with the observed $\log K_a(H_4SiO_4)_{aq}/\log K_a(SiO_2)_{surf}$ ratio. Similar calculations on octahedral species, such as [6]Al^{3+} and [6]Fe^{3+}, should be made to test whether or not the predicted PAs follow the correlation of aqueous and surface species mentioned in Schindler and Stumm (1987). Alternatively, Sverjensky (1993, 1994) recently showed that a correlation exists for $\log (K_a)_{surf}$ values with the inverse of the dielectric constant, $1/\epsilon$, and that the zero-point-of-charge on a mineral surface can be predicted from $1/\epsilon$ and s/r_{M-OH} (where s = the Pauling bond strength and r_{M-OH} = the cation-OH bond length). If this is the case, surface acidity may be controlled by bulk properties of the mineral.

Our results predict a PA = 777 kJ/mol for the reaction $H_7Si_2O_7 \rightarrow H_6Si_2O_7 + H^+$ with a $6-311+G^{**}//3-21G^{**}$ basis set (Table 2). Rustad and Hay (1994) predicted a value of 695 kJ/mol with analytical potentials in molecular mechanics calculations that is reasonably close to our calculated PA. Nicholas et al. (1992) predicted a PA of 690–880 kJ/mol with ab initio calculations for $H_6Si_2OH \rightarrow H_6Si_2O + H^+$. The consistency of the above values suggests that PAs of terminal Si-O groups may be nearly twice that of Si-OH-Si, consistent with the higher acidities of protonated bridging O atoms in comparison with silanols (e.g., Engelhardt et al. 1987). We conclude that under conditions in which Si-O or Si-OH groups dominate a mineral surface, the bonds that attach the Si^{4+} to the bulk mineral are unlikely to be protonated.

Proton affinities in model albite clusters

The $6-311+G^{**}//3-21G^{**}$ calculations give PAs of 2004 and 1317 kJ/mol for $(Si_3)Al-OH$ and $(Si_3)Al-OH_2$, respectively. We estimate the cluster-size and basis-set effects combined to be approximately 5% in these calculated PAs, because MP2 $6-31G^*$ calculations yield a PA of 2097 kJ/mol for the reaction $(H_4AlO_4)^- \rightarrow (H_3AlO_4)^{2-} + H^+$ and 1363 kJ/mol for the reaction $H_5AlO_4 \rightarrow [Al-$ $(OH)_4]^- + H^+$. The ΔPAs of 93 kJ/mol for $(Si_3)Al-OH$ and $(Si_3)Al-OH_2$ and 46 kJ/mol for $[Al(OH)_4]^-$ and H_5AlO_4 are significant. However, the ratios of the PAs are similar in both calculations (1.52 vs. 1.53), suggesting that the relative reactivities are similar in both clusters.

Substitution of Al^{3+} for Si^{4+} in one of the second-nearest-neighbor positions of $(Si_3)Si-OH$ to form $(Si_2Al)Si-OH$ increases the calculated PA of the Q^3 Si-OH group by 378 to 1807 kJ/mol (Table 2). The excess electronic charge on the $(Si_2Al)Si-OH$ molecule accounts for most of the increase in PA. This result is consistent with the experimental data, which show decreasing acidity of OH groups in zeolites as the number of Al^{3+} second-nearest neighbors increases (Gil et al. 1994). However, we note that the $(Si_2Al)Si-OH$ molecule is not charge balanced with Na^+, as would be the case in albite, for instance. The effect of Na^+ would be to lower the PA of the molecule, because the calculated PA of $Na^+[(HSi_2Al)Si-OH]$ is 1468 kJ/mol. Only a 40 kJ/mol increase in the PA of albite Si-OH groups over quartz Si-OH groups is predicted in this case. The Na^+ effect in our model molecules may overestimate the effect charge balancing Na^+ would have in a crystal structure because the Na^+ is in a lower coordination state and more tightly bound to one tetrahedron in the model molecule than in minerals such as albite. Because our model molecule overestimates the Na^+ effect, the maximum reduction in PA for $(Si_2Al)Si-OH$ would be 340 kJ/mol. This estimate is close to the charge-compensation effect on PA calculated by Kramer and van Santen (1993). Such a reduction would give a value of PA for Si-OH on an albite surface similar to that for Si-OH on a quartz surface [i.e., $1807 - 340 = 1467$ kJ/mol compared to 1429 kJ/mol for $(Si_3)Si-OH$; Table 2]. We conclude that PAs of Si-OH groups on albite surfaces could range 400 kJ/mol from near the value calculated for $(Si_3)Si-OH$ to the value calculated for $(Si_2Al)Si-OH$. If this is the case, it becomes difficult to model aluminosilicate surface protonation in terms of mixtures of the component oxides because second-nearest-neighbor effects are significant.

The charge-balancing cation effect on PAs can be estimated by comparing the reactions $(HSi)_3Al-OH \rightarrow (HSi)_3Al-O + H^+$ and $Na^+(HSi)_3Al-OH \rightarrow Na^+(HSi)_3Al-O + H^+$ (Table 2). The PAs of 2028 and 1637 kJ/mol indicate a significant effect on the calculated PA because of the presence of Na^+. [Note that the difference in PAs between $(Si_3)Al-OH$ and $Na^+(HSi_3)Al-OH$ is not the result of substitution of H^- for $(OH)^-$ on the external Si tetrahedra because $(Si_3)Al-OH$ and $(HSi_3)Al-OH$ have nearly equivalent PAs (i.e., 2004 and 2028 kJ/mol; Table 2).] Because Na^+ in the model molecules overestimates the effect of charge balancing Na^+ in crystals, as mentioned above, we consider the PAs listed for $(Si_3)Al-OH$ and $Na^+(HSi_3)Al-OH$ in Table 2 to be estimates of the maximum and minimum values for Al-OH proton affinities on the surface of albite.

As mentioned in the Methods section, the $(Si_3)Al-O$ molecule has a lower potential energy if one H^+ jumps from an Si-OH group to the Al-O group to form Al-OH

and Si-O. This is reflected in the ΔE value of -212 kJ/mol for $(Si_3)Al-O \rightarrow (Si_2Al)Si-O$ (Table 2). Switching the position of the Al^{3+} from a Q^3 to a Q^1 site is not responsible for the large energy decrease because ΔE between $(Si_3)Al-OH \rightarrow (Si_2Al)Si-OH$ is only -16 kJ/mol (Table 2). (Note, however, that Al^{3+} does slightly favor the less polymerized site in this case.) The lower potential energy of the Al-OH + Si-O configuration vs. the Al-O + Si-OH configuration is consistent with the observed higher acidities of surface Si-OH in comparison with Al-OH (Schindler and Stumm 1987).

For the reaction $H_7SiAlO_7 \rightarrow (H_6SiAlO_7)^- + H^+$, PA $= 1301$ kJ/mol (Table 2), which falls within the experimental range of 1188–1330 kJ/mol in zeolites (Datka et al. 1988). Our calculated value is also close to the best theoretical estimate of 1234 kJ/mol by Brand et al. (1993) for Si-O-Al linkages in zeolites. Hence, formation of an Al-OH bond is predicted to be more stable by ~700 kJ/mol than an Si-OH-Al linkage; and the formation of an Al-OH$_2$ group is as energetically favorable as an Si-OH-Al linkage, within the accuracy of these calculations (Table 2). Again, addition of Na^+ to these molecules lowers the calculated PAs (Table 2). However, the PA of $Na^+[(HSi_3)Al-OH]$ is still more stable by ~700 kJ/mol than an $Na^+(Al-OH-Si)$ linkage (1637 vs. 954 kJ/mol), and the PA of $Na^+[(HSi_3)Al-OH_2]$ remains close to that of $Na^+(Al-OH-Si)$ (963 vs. 954 kJ/mol). On a mineral surface, such as an albite crystal, these results translate into protonation of any Al-O sites before Al-OH or Si-O-Al sites become protonated. Once Al-O sites are no longer available, however, Al-OH and Si-O-Al sites should protonate in roughly equal proportions.

Vibrational frequencies of surface sites

Table 3 contains T-O, T-OH, T-OH$_2$, and O-H vibrational frequencies and intensities calculated for the molecules in this study. The calculated Si-OH stretching frequency of 940 cm^{-1} is fairly close to the 970 cm^{-1} value determined for Q^3 Si-OH stretching by curve-fitting Raman spectra of hydrous SiO_2 glasses (Mysen and Virgo 1986). The Si-OH and Al-OH stretching frequencies (940 and 805 cm^{-1}, respectively) straddle the reported value of 880 cm^{-1} for T-OH stretching in hydrous aluminosilicate glasses (Mysen et al. 1980). Addition of Na^+ to the $(HSi)_3Al-OH$ molecule increases the value of the Q^3 Al-OH stretch to 883 cm^{-1}, perhaps fortuitously close to the Al-OH stretching frequency of 880 cm^{-1} in hydrous aluminosilicate glasses (Sykes and Kubicki 1993). According to the calculated results, Si-OH stretches are relatively more IR active and Al-OH stretches more Raman active. Al-OH$_2$ stretches are predicted to occur at the much lower frequencies of 582 and 533 cm^{-1} with a moderate IR intensity and weak Raman activity (Table 3).

O-H stretching frequencies of 3806 and 3802 cm^{-1} (Table 3) calculated for Q^3 Si-OH molecules are somewhat higher than the 3740 cm^{-1} value assigned to free (i.e., non–hydrogen bonded) surface silanol groups (Fripiat 1982). Hydrogen bonding to the Si-OH and Al-OH groups in these model molecules is insignificant because

TABLE 3. Calculated vibrational frequencies (scaled by 0.89) and intensities for the T-O, T-OH, T-OH$_2$, and O-H modes of the molecules in this study

Molecule	T-O, T-OH, or T-OH$_2$			O-H		
	ν (cm^{-1})	IR (km/mol)	Raman (Å⁴/mol)	ν (cm^{-1})	IR (km/mol)	Raman (Å⁴/mol)
(Si$_3$)Si-O	1155	695	7.9			
(Si$_3$)Si-OH	940 (970)ª	292	2.1	3806 (3740–3750)ᵇ	331	0.4
(Si$_2$Al)Si-O	1170	272	4.6			
Na⁺(HSi$_2$Al)Si-O	1219	466	1.5			
(Si$_2$Al)Si-OH	947	126	1.4	3802	73	56.8
Na⁺(HSi$_2$Al)Si-OH	935	673	6.8	3810	159	64.9
(Si$_3$)Al-OH	805	14	8.4	3768 (3760–3780)ᶜ	32	70.0
(HSi$_3$)Al-OH	793	258	4.9	3780	6	100.2
Na⁺(HSi$_3$)Al-OH	883 (880)ᵈ	125	1.6	3900 (3760–3780)ᶜ	100	81.7
(Si$_3$)Al-OH$_2$ᵉ	582	132	3.8	3339	1215	38.0
(Si$_3$)Al-OH$_2$ᶠ				3256	515	65.0
(Si$_3$)Al-OH$_2$ᵍ				1632	124	3.1
Na⁺(HSi$_3$)Al-OH$_2$	533	47	0.6	3735	291	29.2
Na⁺(HSi$_3$)Al-OH$_2$				3620	192	42.8
Na⁺(HSi$_3$)Al-OH$_2$ᵍ				1592 (1662)ʰ	189	3.2
Si(OH)Si				3600	336	29.2
Al(OH)Si				3640	251	31.2
Na⁺Al(OH)Si				3659 (3610)ⁱ	286	37.9
[6]Al-(OH)ʲ·ᵏ				3926	259	56.7

Note: Experimental values in parentheses; a = Mysen and Virgo (1986), b = Fripiat (1982), c = Knözinger and Ratnasamy (1978), d = Sykes and Kubicki (1993), e = H···O2 bond of 1.71 Å, f = H···O2 bond of 1.73 Å, g = H-O-H bending mode, h = Morterra et al. (1976), i = Datka et al. (1988), j = Kubicki et al. (1995b), and k = [(H$_2$O)$_5$AlOH]$^{2+}$.

the H···O2 distance in each case is >3 Å, which is beyond the range in which hydrogen bonding has a large effect on O-H stretching frequencies in aluminosilicate molecules (Kubicki et al. 1993a). The O-H stretch associated with the Q^3 Si^{4+} cation does not change significantly with substitution of Al^{3+} in a second-nearest-neighbor position or addition of Na^+. The OH in (Si$_3$) Al-OH is predicted to vibrate at 3768 cm^{-1}, which falls within the experimental ν(OH) stretch range of 3760–3780 cm^{-1} found on mineral surfaces with Al^{3+} in tetrahedral coordination (Knözinger and Ratnasamy 1978). In the (HSi$_3$)Al-OH and Na⁺(HSi$_3$)Al-OH molecules, ν(OH) = 3780 and 3900 cm^{-1}, respectively. O-H bonded to Al is predicted to be a relatively weak IR absorber and strong Raman absorber; whereas, the opposite is true of the O-H associated with Si. This prediction points out the need to measure both the IR and Raman spectra of minerals to characterize the surface species.

O-H stretches in (Si$_3$)Al-OH$_2$ are at 3256 and 3339 cm^{-1} (Table 3), approximately 400–500 cm^{-1} lower in frequency than those in the Al-OH group. This decrease is caused by the higher coordination number of O atoms in (Si$_3$)Al-OH$_2$ and the formation of hydrogen bonds of 1.71 and 1.73 Å, respectively. In comparison, O-H stretching frequencies are predicted to be 3620 and 3735 cm^{-1} in Na⁺(HSi$_3$)Al-OH$_2$ (Fig. 2b), where no hydrogen

bonding occurs with regard to the $Al\text{-}OH_2$ group. Hydrogen bonded O-H vibrations in $Al\text{-}OH_2$ groups could account for the broad bands observed between 3000–3800 cm^{-1} in infrared spectra of hydrated feldspars (Koretsky et al., in preparation). O-H stretching modes in $(Si_3)Al\text{-}OH_2$ and $Na^+(HSi_3)Al\text{-}OH_2$ are calculated to be both IR and Raman active. The H-O-H bending mode calculated at 1632 cm^{-1} is close to that observed for adsorbed molecular H_2O on alumina surfaces (1660 cm^{-1}; Morterra et al. 1976) and in aluminosilicate glasses at 1635 cm^{-1} (Silver and Stolper 1989).

O-H stretching frequencies on bridging O atoms range from 3600 to 3660 cm^{-1} according to our calculations (Table 3). This range overlaps the value of 3609 measured for the NaH-ZSM-5 zeolite (Datka et al. 1988). Such good agreement between the model-molecule values and that measured in a crystal structure lends support to our assumption that vibrational frequencies are generally controlled by short-range structure surrounding the vibrating group. Furthermore, because $\nu(OH)$ in zeolites correlates with the PAs and acidity of the T-OH-T sites (Datka et al. 1988), the correspondence of the O-H vibrational frequency also suggests that relative acidity of mineral-surface sites is accurately modeled by our calculations. Lower vibrational frequencies of the T-OH-T and $T\text{-}OH_2$ OH groups are consistent with our earlier interpretations of relative acidity on the basis of energetics.

DISCUSSION

The consistent agreement between observed vibrational frequencies in condensed phases and those calculated for our model molecules indicates that the MO approach employed in this study is a valuable tool for interpreting vibrational spectra of minerals and glasses. Correspondence between the calculated silanol $\nu(O\text{-}H)$ stretching frequency in $(Si_3)Si\text{-}OH$ and $(Si_2Al)Si\text{-}OH$ and the observed frequencies on silica and albite surfaces (Koretsky et al., in preparation) confirms the idea that Q^3 Si-OH species are formed near neutral pH (Schindler and Stumm 1987). Comparison of the calculated O-H stretching frequencies in $(Si_3)Al\text{-}OH$ and $(Si_3)Al\text{-}OH_2$ with the measured infrared spectra of feldspar (Fripiat 1982; Koretsky et al., in preparation) suggests that Q^3 $Al\text{-}OH_2$ could be the dominant terminal species of Al^{3+} formed near neutral pH, also consistent with measured pK_a values (Schindler and Stumm 1987). Theoretical vibrational spectra of the other species in this study can be used as a guide for interpreting vibrational spectra of silica and feldspar surfaces hydrated in a range of pH conditions.

Although PAs alone grossly overestimate equilibrium constants because of neglect of solvation and entropy effects, calculated PA values can correlate well with experimental pK_a values because the errors caused by neglect of solvation and entropy are systematic and tend to be constant along a protonation series (Rustad and Felmy 1995; Kubicki et al. 1995a). The consistency of the PAs calculated in this study with experimental protonation

behavior also leads us to conclude that reaction energetics obtained from MO theory can be useful in interpreting surface reactions. For example, a comparison of experimental and theoretical results reveals similarities for silica protonation behavior. The reaction $SiO^- + H^+ \rightarrow Si\text{-}OH$ on quartz and silica gels has an experimental pK_a^s of 6.7 (Schindler and Gamsjäger 1972). Our corresponding PA values are 1429 and 1665 kJ/mol for $SiO^- + H^+ \rightarrow Si\text{-}OH$ and $(OH)^- + H^+ \rightarrow H_2O$, respectively. The PA values of Si-OH and H_2O are relatively similar in comparison with the large range of values calculated (i.e., 700–2000 kJ/mol; Table 2), suggesting a value of $pK_a(SiO_2)_{surf}$ just below neutral pH for surface silanol groups, as is observed.

Another objective of this study was to determine if Si-OH groups on silica surfaces have PAs similar to those of Si-OH groups on feldspar surfaces because some researchers have used component oxides to model aluminosilicate protonation (e.g., Parks 1967). Although the PA of an Si-OH group on an albite surface could be equal to that on a quartz surface according to our calculations (Table 2), the range of PA values for Si-OH on an albite surface should be much greater, with a higher average value than that for a quartz surface. Thus, Si-OH may form at higher pH on feldspars than on quartz. Because the same argument holds true for bridging O sites, Si-O-Si and Si-O-Al, the rate of dissolution of Si in acid solution should be greater in feldspars than in quartz because T-OH-T linkages are more readily broken than T-O-T linkages (Xiao and Lasaga 1995).

Next, we turn our attention toward the interpretation of dissolution mechanisms on the basis of calculated structural changes with protonation and relative PAs between various O atoms in our model molecules. MO calculations predicted that both $Si\text{-}O_{br}$ and $Al\text{-}O_{br}$ bonds tend to strengthen as surface T-O bonds are protonated. However, dissolution rates of feldspars in aqueous solution do not monotonically decrease with decreasing pH; dissolution rates increase from a minimum at neutral pH as the solution becomes more acidic or basic (e.g., Blum and Lasaga 1988; Hellmann et al. 1990). Hence, we examined the likely sequence of elementary reactions that may occur at aluminosilicate mineral-water interfaces under basic, neutral, and acidic conditions.

Increasing dissolution rates with increasing pH under basic conditions are readily understandable in terms of the calculated results of weakened $T\text{-}O_{br}$ bonds as Si-OH and $Al\text{-}OH_2$ groups are deprotonated to form $Si\text{-}O^-$, Al-OH, and $Al\text{-}O^-$ groups. Water molecules are able to form stronger hydrogen bonds to bridging O atoms in these weakened T-O-T linkages because of the increase in local charge and the decrease in bond strength to the bridging O atom (Gibbs et al. 1981). Thus, hydrolysis should require less energy. This conclusion is consistent with the experimental interpretation by Brady and Walther (1989) of increasing dissolution rates in basic pH. Lengthened $Al\text{-}O_{br}$ bonds may also allow $(OH)^-$ or H_2O to attack and bond to Al^{3+} more readily. On the basis of NMR spectra,

Bunker et al. (1988) suggested that fivefold- and sixfold-coordinated species do not form readily from Q^3 species, so this type of nucleophilic attack may occur only at sites where Q^2 T-OH$_2$ species have already formed (i.e., corner sites on the mineral surface).

The calculated strengthening of T-O$_{br}$ bonds in (Si$_3$)Al-OH$_2$ and (Si$_2$Al)Si-OH in comparison with (Si$_3$)Al-OH and (Si$_2$Al)Si-O$^-$ helps to explain the observed feldspar dissolution-rate minimum near neutral pH. According to our calculations, Si-OH and Al-OH$_2$ should be the dominant OH species on feldspar surfaces near neutral pH. The shorter and stronger the Al-O$_{br}$ bond, the more energy is required to hydrolyze the Al-O-Si linkage (a step in the dissolution process; Xiao and Lasaga 1995). In addition, the concentration of H$^+$ in the neutral solution is so low that proton attacks on Si-O-Al linkages are not common.

Increasing dissolution rates with increasing acidity can be explained by protonation of bridging O atoms as a direct competition with terminal OH groups for protons from H$_3$O$^+$ (Hellmann et al. 1990). Al-OH$_2$ groups cannot effectively compete for additional protons in comparison with Al-O-Si because the PA of Al-OH $\rightarrow$ Al-OH$_2$ is roughly equal to the PA of Al-O-Si $\rightarrow$ Al-OH-Si (1317 vs. 1301 kJ/mol without Na$^+$ and 963 vs. 954 kJ/mol with Na$^+$; Table 2). In fact, MO calculations on the molecule [(OH)$_3$Al-(OH$_3$)]$^+$ predict that addition of a third proton to the terminal Al-OH$_2$ group would break the Al-OH$_2$ bond to form Al(OH)$_3$ + H$_3$O$^+$ (Kubicki et al. 1996). This prediction is similar to the interpretation of Bunker et al. (1988) regarding formation of trigonal B in leached sodium borosilicate glasses. T-O$_{br}$ bonds involved in Al-OH-Si linkages are significantly lengthened (Brand et al. 1993; Sykes and Kubicki 1993; Xiao and Lasaga 1995); hence, the dissolution rate increases as a function of decreasing pH. A similar process should occur in quartz because the PA values of Si-OH-Si and Si-(OH$_2$)$^+$ are nearly equivalent to each other (777 vs. 776 kJ/mol; Table 2). However, on quartz the proton transfer would occur at lower pH because the Si^{4+} species have PAs that are lower than those of the corresponding Al^{3+} species (Table 2).

We note that our calculations predict gas-phase PA values of 1665 and 694 kJ/mol for H$_2$O and H$_3$O$^+$, respectively (Table 2), which are close to the experimental values (Lias et al. 1988). Hence, H$_3$O$^+$ would give up a proton to Si-O and Al-O, Al-OH, and Al-O-Si groups; whereas, H$_2$O is likely to protonate only Si-O and Al-O groups on albite surfaces. The calculated PAs of [(OH)$_3$Si(OH$_2$)]$^+$ and (H$_7$Si$_2$O$_7$)$^+$ are 776 and 777 kJ/mol, respectively (Table 2), suggesting that protons would be distributed fairly evenly between these two groups and H$_3$O$^+$ under acidic conditions where the Al-OH$_2$ and Al-OH-Si groups are fully protonated (i.e., pH < 2).

Another possible mechanism involved in the dissolution reaction is the attack of an H$_2$O molecule against Al^{3+} opposite the Al-OH$_2$ bond to form a pentacoordinated Al species (Furrer and Stumm 1986). Figure 2 illustrates nearly coplanar arrangements of the bridging O atoms in (Si$_3$)Al-OH$_2$ and Na$^+$(HSi$_3$)Al-OH$_2$. In these structures, an Al^{3+} cation could directly form a fifth bond with an H$_2$O molecule. Pentacoordinated Si^{4+} has been suggested as a possible reaction intermediate in the dissolution of quartz under basic conditions (Kubicki et al. 1993b), and pentacoordinated Al^{3+} is more likely to form because of the larger ionic radius of Al^{3+} in comparison with Si^{4+}. However, the pentacoordinated Al^{3+} reaction intermediate would form under neutral to acidic conditions where Al-OH$_2$ groups are prevalent.

Polarization and weakening of cation-bridging O bonds by the formation of X-OH$_2$ groups has been used to explain increasing dissolution rates with lower pH values (e.g., Furrer and Stumm 1986; Wieland et al. 1988). According to our calculations, this does not occur on albite surfaces if Al^{3+} remains in tetrahedral coordination. Bond weakening does occur, however, if chemisorption of the H$_2$O leads to a pentacoordinated Al^{3+} (Kubicki and Sykes 1995). As mentioned earlier, coordination states higher than tetrahedral may not form from Q^4 and Q^3 cations (Bunker et al. 1988), but Hellmann et al. (1990) noted that an increase in coordination state probably occurs during the dissolution reaction if the Al species in acid pH solutions is octahedrally coordinated [e.g., Al^{3+} · 6(H$_2$O)]. We conclude that direct nucleophilic attack by H$_2$O is probable after at least two Al-OH$_2$ groups have formed on a given cation, so a second Al-O-Si linkage in a species such as that depicted in Figure 2 may need to be hydrolyzed before the coordination change occurs. Once a pentacoordinated Al^{3+} reaction intermediate has formed on the surface, the remaining Al-O$_{br}$ bonds are more readily hydrolyzed, and attack by another H$_2$O molecule leads to the formation of Al$_{aq}^{3+}$.

REFERENCES CITED

Balistrieri, L.S., and Murray, J.W. (1984) Marine scavenging: Trace metal adsorption by interfacial sediment from MANOP site H. Geochimica et Cosmochimica Acta, 48, 921–929.

Blum, A.E., and Lasaga, A.C. (1988) Role of surface speciation in the low-temperature dissolution of minerals. Nature, 331, 431–433.

Boehm, H.P. (1966) Chemical identification of surface groups. Advances in Catalysis, 12, 179–274.

Brady, P.V., and Walther, J.V. (1989) Controls on silicate dissolution rates in neutral and basic pH solutions at 25 °C. Geochimica et Cosmochimica Acta, 53, 2823–2830.

Brand, H.V., Curtiss, L.A., Iton, L.E. (1993) Ab initio molecular orbital cluster studies of the zeolite ZSM-5: 1. Proton affinities. Journal of Physical Chemistry, 97, 12773–12782.

Bunker, B.C., Tallant, D.R., Headley, T.J., and Turner, G.L. (1988) The structure of leached sodium borosilicate glass. Physics and Chemistry of Glasses, 29, 106–120.

Datka, J., Boczar, M., and Rymarowicz, P. (1988) Heterogeneity of OH

groups in NAH-ZSM-5 zeolite studies by infrared spectroscopy. Journal of Catalysis, 114, 368–376.

Dowty, E. (1993) Atoms: A computer program for displaying atomic structures. Kingsport, Tennessee.

Engelhardt, G., Jerschkewitz, H.-G., Lohse, U., Sarv, P., Samoson, A., and Lippmaa, E. (1987) 500 Mhz ^{1}H MAS NMR studies of dealuminated HZSM-5 zeolites. Zeolites, 7, 289–292.

Fleischer, U., Kutzelnigg, W., Bleiber, A., and Sauer, J. (1993) ^{1}H NMR chemical shift and intrinsic acidity of hydroxyl groups: Ab initio calculations on catalytically active sites and gas-phase molecules. Journal of the American Chemical Society, 115, 7833–7838.

Fripiat, J.J. (1982) Silanol groups and properties of silica surfaces. In J.S. Falcone, Ed., Soluble silicates, p. 165–184. ACS Symposium Series 194.

Frisch, M.J., Trucks, G.W., Head-Gordon, M., Gill, P.M.W., Wong, M.W., Foresman, J.B., Johnson, B.G., Schlegel, H.B., Robb, M.A., Replogle, E.S., Gomperts, R., Andres, J.L., Raghavachari, K., Binkley, J.S., Gonzalez, C., Martin, R.L., Fox, D.J., Defrees, D.J., Baker, J., Stewart, J.J.P., and Pople, J.A. (1992) Gaussian 92 Revision C, Gaussian, Inc. Pittsburgh, Pennsylvania.

Furrer, G., and Stumm, W. (1986) The coordination chemistry of weathering: I. Dissolution kinetics of δ-Al$_2$O$_3$ and BeO. Geochimica et Cosmochimica Acta, 50, 1847–1860.

Geisinger, K.L., Gibbs, G.V., and Navrotsky, A. (1985) A molecular orbital study of bond length and angle variations in framework structures. Physics and Chemistry of Minerals, 11, 266–283.

Gibbs, G.V., Meagher, E.P., Newton, M.D., and Swanson, D.K. (1981) Comparison of experimental and theoretical bond length and angle variations for minerals and inorganic solids and molecules. In M. O'Keeffe and A. Navrotsky, Eds., Structure and bonding in crystals, p. 195–225. Academic, New York.

Gil, B., Broclawik, E., Datka, J., and Klinowski, J. (1994) Acidic hydroxyl groups in zeolites X and Y: A correlation between infrared and solid-state NMR spectra. Journal of Physical Chemistry, 98, 930–933.

Hehre, W.J., Radom, L., Schleyer, P.R., and Pople, J.A. (1986) Ab initio molecular orbital theory, 548 p. Wiley Interscience, New York.

Hellmann, R., Eggleston, C.M., Hochella, M.F., and Crerar, D.A. (1990) The formation of leached layers on albite surfaces during dissolution under hydrothermal conditions. Geochimica et Cosmochimica Acta, 54, 1267–1281.

Hochella, M.F., and White, A.F. (1990) Mineral-water interface geochemistry, 603 p. Mineralogical Society of America, Washington, DC.

Kirkpatrick, R.J. (1988) MAS NMR spectroscopy of minerals and glasses. In Mineralogical Society of America Reviews in Mineralogy, 18, 341–403.

Knözinger, H., and Ratnasamy, P. (1978) Catalytic aluminas: Surface models and characterization of surface sites. Catalysis Reviews—Science and Engineering, 17, 31–70.

Kramer, G.J., and van Santen, R.A. (1993) Theoretical determination of proton affinity differences in zeolites. Journal of the American Chemical Society, 115, 2887–2897.

Kubicki, J.D., and Sykes, D. (1993) Molecular orbital calculations of vibrations in three-membered aluminosilicate rings. Physics and Chemistry of Minerals 19, 381–391.

Kubicki, J.D., Sykes, D., and Rossman, G.R. (1993a) Calculated trends of OH infrared stretching vibrations with composition and structure in aluminosilicate molecules. Physics and Chemistry of Minerals, 20, 425–432.

Kubicki, J.D., Xiao, Y., and Lasaga, A.C. (1993b) Theoretical reaction pathways for the formation of [Si(OH)$_5$]$^{1-}$ and the deprotonation of orthosilicic acid in basic solution. Geochimica et Cosmochimica Acta, 57, 3847–3853.

Kubicki, J.D., Apitz, S.E., and Sykes, D. (1995a) Molecular orbital calculations of aqueous-phase aluminum: Aluminum hydrolysis and organic ligand complexation. Abstracts with Programs, GSA Annual Meeting, 27, A311.

Kubicki, J.D., Blake, G.A., and Apitz, S.E. (1995b) G2 theory calculations on [H$_3$SiO$_4$]$^-$, [H$_4$SiO$_4$], [H$_3$AlO$_4$]$^{2-}$, [H$_4$AlO$_4$]$^-$, and [H$_5$AlO$_4$]: Basis set and electron correlation effects on molecular structures, atomic charges, infrared spectra, and potential energies. Physics and Chemistry of Minerals, 22, 481–488.

Kubicki, J.D., and Sykes, D. (1995) Molecular orbital calculations of the vibrational spectra of Q^3 T-(OH) species and the hydrolysis of a three-membered aluminosilicate ring. Geochimica et Cosmochimica Acta, 59, 4791–4794.

Kubicki, J.D., Blake, G.A., and Apitz, S.E. (1996) Molecular orbital models of aqueous aluminum-acetate complexes. Geochimica et Cosmochimica Acta, in press.

Lasaga, A.C. (1992) Ab initio methods in mineral surface reactions. Reviews in Geophysics, 30, 269–303.

Lias, S., Bartmess, J.E., Liebman, J.F., Holmes, J.L., Levine, R.D., and Mallard, W.G. (1988) Journal of physical chemistry reference data, 17, Supplement, 1.

Møller, C., and Plesset, M.S. (1934) Note on an approximation treatment for many-electron systems. Physical Review, 46, 618–622.

Morterra, C., Ghiotti, G., Garrone, E., and Boccuzzi, F. (1976) Infrared spectroscopic characterization of the α-alumina surface. Journal of the Chemical Society, Faraday Transactions, 72, 2722–2734.

Mysen, B.O., Virgo, D., Harrison, W., and Scarfe, C.M. (1980) Solubility mechanisms of H$_2$O in silicate melts at high pressures and temperatures: A Raman spectroscopic study. American Mineralogist, 65, 900–914.

Mysen, B.O., and Virgo, D. (1986) Volatiles in silicate melts at high pressure and temperature: 1. Interaction between OH groups and Si^{4+}, Al^{3+}, Ca^{2+}, Na$^+$ and H$^+$. Chemical Geology, 57, 303–331.

Nicholas, J.B., Winans, R.E., Harrison, R.J., Iton, L.E., Curtiss, L.A., and Hopfinger, A.J. (1992) Ab initio molecular orbital study of the effects of basis set size on the calculated structure and acidity of hydroxyl groups in framework molecular sieves. Journal of Physical Chemistry, 96, 10247–10257.

O'Keeffe, M., Domenges, B., and Gibbs, G.V. (1985) Ab initio molecular orbital calculations on phosphates: Comparison with silicates. Journal of Physical Chemistry, 89, 2304–2309.

Parks, G.A. (1967) Aqueous surface chemistry of oxides and complex oxide minerals: Isoelectric point and zero point of charge. In Equilibrium Concepts in Natural Water Systems, 67, Advances in Chemistry Series, American Chemical Society, p. 121–160.

Paukshtis, E.A., and Yurchenko, E.N. (1983) Use of IR spectroscopy in studies of acid-basic properties of heterogeneous catalysts. Uspekhi Khimii, 52, 426–454.

Pople, J.A., Schlegel, H.B., Krishnan, R., Defrees, D.J., Binkley, J.S., Frisch, M.J., Whiteside, R.A., Hout, R.F., and Hehre, W.J. (1981) Molecular-orbital studies of vibrational frequencies. International Journal of Quantum Chemistry: Quantum Chemistry Symposium, 15, 269–278.

Rustad, J.R., and Hay, B.P. (1994) A molecular dynamics study of solvated orthosilicic acid and orthosilicate anion using parameterized potentials. Geochimica et Cosmochimica Acta, 59, 1251–1257.

Rustad, J.R., and Felmy, A.R. (1995) Crystallographic heterogeneity of goethite surfaces. Eos, 76, S101.

Sauer, J., and Hill, J.R. (1994) The acidity of surface silanol groups: A theoretical estimate based on ab-initio calculations on a model surface. Chemical Physics Letters, 218, 333–337.

Schindler, P.W., and Gamsjäger, H. (1972) Acid-base reactions of the TiO$_2$ (Anatase)-water interface and the point of zero charge of TiO$_2$ suspensions. Kolloid Zeitschrift Polymere, 250, 759–763.

Schindler, P.W., and Stumm, W. (1987) The surface chemistry of oxides, hydroxides, and oxide minerals. In W. Stumm, Ed., Aquatic surface chemistry: Chemical processes at the particle-water interface, p. 83–100. Wiley, New York.

Schulthess, C.P., and Huang, C.P. (1991) Humic and fulvic acid adsorption by silicon and aluminum oxide surfaces on clay minerals. Soil Science Society of America Journal, 55, 34–42.

Sharma, S.K., Yoder, H.S., Jr., and Matson, D.W. (1988) Raman study of some melilites in crystalline and glassy states. Geochimica et Cosmochimica Acta, 52, 1961–1967.

Silver, L., and Stolper, E.M. (1989) Water in albitic glasses. Journal of Petrology, 30, 667–709.

Stave, M.S., and Nicholas, J.B. (1993) Density functional study of cluster models of zeolites: 1. Structure and acidity of hydroxyl groups in disiloxane analogs. Journal of Physical Chemistry, 97, 9630–9641.

Sverjensky, D.A. (1993) Physical surface-complexation models for sorption at the mineral-water interface. Nature, 364, 776–780.

——— (1994) Zero-point-of-charge prediction from crystal chemistry and solvation theory. Geochimica et Cosmochimica Acta, 58, 3123–3129.

Sykes, D., and Kubicki, J.D. (1993) A model for H_2O solubility mechanisms in albite melts from infrared spectroscopy and molecular orbital calculations. Geochimica et Cosmochimica Acta, 57, 1039–1052.

——— (1996) Four-membered rings in silica and aluminosilicate glasses. American Mineralogist, 81, 265–272.

Westall, J.C. (1987) Adsorption mechanisms in aquatic surface chemistry. In W. Stumm, Ed., Aquatic surface chemistry: Chemical processes at the particle-water interface, p. 3–32. Wiley, New York.

Wieland, E., Werhli, B., and Stumm, W. (1988) The coordination chemistry of weathering: III. A potential generalization on dissolution rates of minerals. Geochimica et Cosmochimica Acta, 52, 1969–1981.

Xiao, Y., and Lasaga, A.C. (1995) Ab initio quantum mechanical studies of the kinetics and mechanisms of silicate dissolution: $H^+(H_3O^+)$ catalysis. Geochimica et Cosmochimica Acta, 58, 5379–5400.

Zachara, J.M., Resch, C.T., and Smith, S.C. (1994) Influence of humic substances on Co^{2+} sorption by a subsurface mineral separate and its mineralogical components. Geochimica et Cosmochimica Acta, 58, 553–566.